Sensing Polycyclic Aromatic Hydrocarbons with Dithiocarbamate-Functionalized Ag Nanoparticles by Surface-Enhanced Raman Scattering

ARTICLE *in* ANALYTICAL CHEMISTRY · FEBRUARY 2009

Impact Factor: 5.64 · DOI: 10.1021/ac801709e · Source: PubMed

4 AUTHORS, INCLUDING:

Luca Guerrini
Medcom Advance SA
43 PUBLICATIONS **759** CITATIONS
SEE PROFILE

José Vicente García-Ramos
Spanish National Research Council
177 PUBLICATIONS **3,794** CITATIONS
SEE PROFILE

S. Sanchez-Cortes
Spanish National Research Council
197 PUBLICATIONS **4,204** CITATIONS
SEE PROFILE

Anal. Chem. **2009,** *81,* 953–960

Sensing Polycyclic Aromatic Hydrocarbons with Dithiocarbamate-Functionalized Ag Nanoparticles by Surface-Enhanced Raman Scattering

Luca Guerrini, José V. Garcia-Ramos, Concepción Domingo, and Santiago Sanchez-Cortes*

Instituto de Estructura de la Materia, CSIC, Serrano, 121, 28006-Madrid, Spain

Trace detection of polycyclic aromatic hydrocarbons is reported in this work on dithiocarbamate calix[4]arene functionalized Ag nanoparticles by using surface-enhanced Raman scattering (SERS). SERS spectra informed about the existence of the pollutant by measuring its characteristic fingerprint vibrational features. In addition, SERS revealed important structural information from both the host and the analyte which was crucial to understand and deduce the host−guest interaction mechanism. The effectiveness of this system was checked for a group of PAHs: pyrene, benzo[*c*]phenanthrene, triphenylene, and coronene. From the analyzed results, the affinity constants and the limit of detection were deduced for each pollutant.

The optical properties of metallic nanoparticles (NPs) have a big scientific and technological importance due to their large absorption cross section and localized surface plasmons (LSP) on their surface.[1,2] The resonant excitation of the LSP leads to enormous enhancement of the electromagnetic field in NPs, which induces an important enhancement of the cross sections in phenomena involving radiation-to-matter interaction, such as the Raman emission from molecules placed in close proximity to the surface. The surface-enhanced Raman scattering (SERS) is a sensitive technique which has been employed in the last years for different kinds of analytical studies.[3,4] However, the near-field character of the surface-enhanced techniques represents a big problem in the application of the SERS technique in trace analysis, since the analyte must be very close to the surface. The higher surface-to-volume ratio as compared to macroscopic metallic materials entails a great importance of the solid−liquid interface surrounding the metal NPs. In fact, the physicochemical characteristics of this interface will determine the analytical applications of NPs as the sensitivity and the selectivity of these materials are directly related to the interface. In this sense, the interface functionalization plays a crucial role in increasing the analytical applicability of NPs.[5,6] An appropriate functionalization of NPs can improve their properties and increase their selectivity, consequently enlarging their applications.

In particular, the combination of the optical properties of nanostructured metal and the advanced chemical properties of self-assembled calixarenes is a subject of great interest, with promising applications in different fields such as nanotechnology, environment, chemical sensing, and so forth.

Calixarenes (CXs) are synthetic cyclooligomers with a "cup-like" shape, capable of size-selective molecular encapsulation. CXs are widely applied as complexing agents for many metals, organic molecules, and drugs.[7] The tuning of the CX recognition properties is feasible by properly changing the groups on the upper and lower rim which, in turn, induces the modification of the chemical properties of the CX and the reshaping of its cavity. The high performance of CXs as hosts make the CXs a special class of subject in the supramolecular chemistry.[8]

In general the molecules which are active in SERS display a certain affinity toward the metal resulting in the necessary approach to the surface. However many other molecules, whose trace detection is of great interest, do not exhibit this affinity and their SERS signal is not detectable. Among the last ones belongs the group of the environmental contaminants polycyclic aromatic hydrocarbons (PAHs).

Polycyclic aromatic hydrocarbons (PAHs) consist of a family of extremely hazardous pollutants mainly formed during the incomplete combustion of coal, oil, and gas or other organic substances such as tobacco or charbroiled meat. Many of them have been reported to be strong carcinogens.[9] These molecules present a common condensed benzene rings structure and show very low affinity for adsorption on a metallic surface, thus limiting the use of surface-enhanced techniques in their detection. Identification and quantification of PAHs in water solution is usually carried out by HPLC with UV−visible, fluorimetric, or amperometric detection or by means of GC/MS or GC/FID and most of them include a preconcentration step. These steps are time-consuming and require great deal of effort, thus making the analysis unsuitable for routine control analysis.

In previous works we reported that CXs with carboethoxy groups in the lower rim can be successfully applied in the

* Corresponding author.

(1) Aroca, R. *Surface-Enhanced Vibrational Spectroscopy*; John Wiley & Sons, Chichester, U.K., 2006.
(2) Moskovits, M. *J. Raman Spectrosc.* **2005**, *36*, 485–496.
(3) Kneipp, K.; Kneipp, H.; Itzkan, I.; Dasari, R. R.; Feld, M. S. *Chem. Rev.* **1999**, *99*, 2957–2975.
(4) Kneipp, J.; Li, X. T.; Sherwood, M.; Panne, U.; Kneipp, H.; Stockman, M. I.; Kneipp, K. *Anal. Chem.* **2008**, *80*, 4247–4251.
(5) Neouze, M. A.; Schubert, U. *Monatsh. Chem.* **2008**, *139*, 183–195.
(6) Niemeyer, C. M. *Angew. Chem., Int. Ed.* **2001**, *40*, 4128–4158.
(7) Billes, F.; Mohammed-Ziegler, I. *Supramol. Chem.* **2002**, *14*, 451–459.
(8) Saadioui, M.; Bohmer, V. *Calixarenes 2001* **2001**, 130–154.
(9) Harvey, R. G. *Polycyclic Aromatic Hydrocarbons*; John Wiley & Sons: New York, 1997.

10.1021/ac801709e CCC: $40.75
Published on Web 01/07/2009

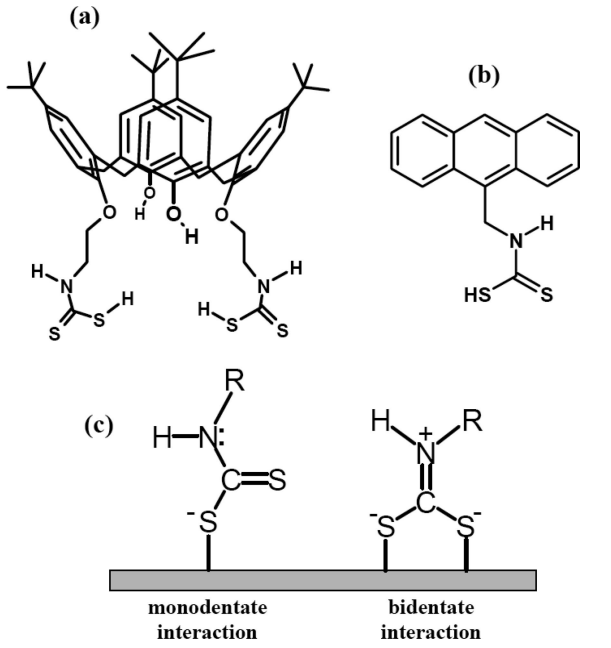

Figure 1. Molecular structures of (a) DTCX and (b) MAMDT. (c) Isomer transition dithiocarbamate form (monodentate interaction) to thioureide form (bidentate interaction) occurring on the metal surface.

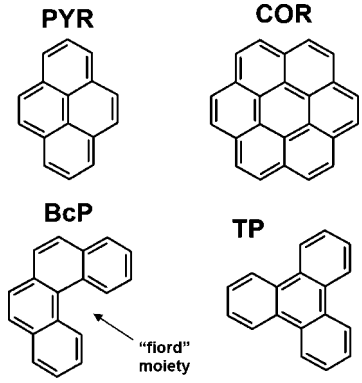

Figure 2. Molecular structures of pyrene (PYR), triphenylene (TP), benzo[*c*]phenanthrene (BcP), and coronene (COR).

detection of PAHs by using the SERS technique.[10−13] The carboethoxy-calix[4]arene derivative displayed a significant selectivity for interaction with PAH molecules bearing four benzene rings, mainly pyrene and benzo[*c*]phenanthrene. In a recent paper we reported the synthesis of a dithiocarbamate (DT) functionalized calix[4]arene (Figure 1a) aimed to improve the affinity of the calixarene host toward the NP surface.[14] DT is able to strongly interact with the surface of metals by forming chelate complexes,[15]

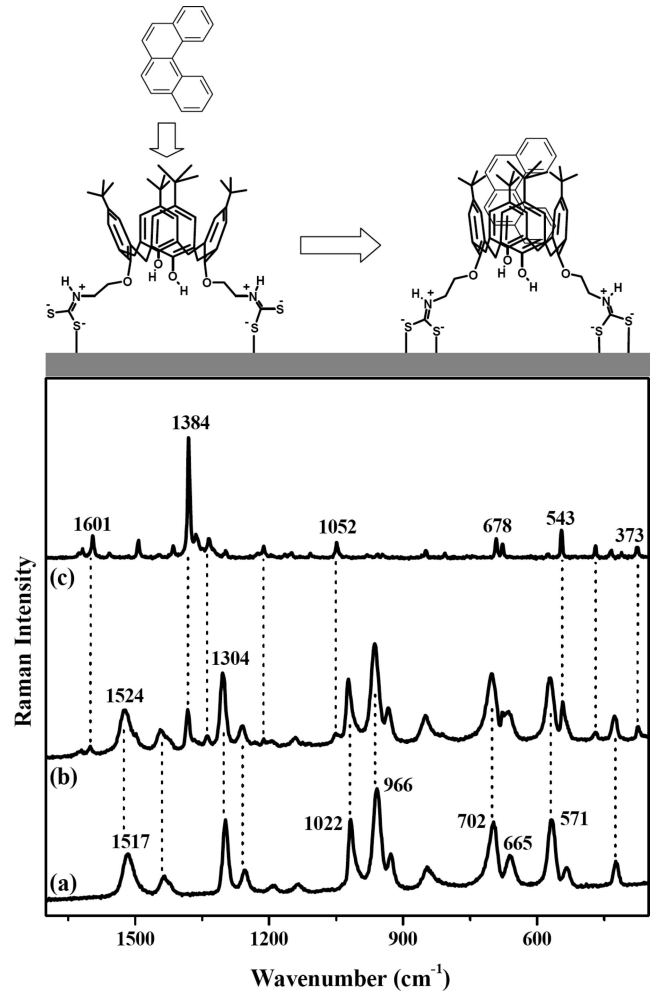

Figure 3. SERS spectra of (a) DTCX (10^{-4} M) and (b) DTCX/BcP ($10^{-4}/10^{-6}$ M). (c) Raman spectrum of BcP in the solid state. Excitation at 785 nm. Top scheme: structural change induced by the interaction of BcP with DTCX, as deduced from the SERS spectra.

as demonstrated in previous studies on the adsorption of DT containing fungicides on nanostructured metal surfaces.[16−18] As a consequence, the use of the dithiocarbamate calixarene (DTCX) as the host leads to an increase of the sensitivity of the sensing system which, in turn, allows for the performing of a quantitative study of the PAHs detection (whereas the previous ones were mainly qualitative). Furthermore, the DT bands are much more sensitive to the different interaction with the metal surface than the ester ones probed in previous works. Therefore, this group provides molecular marker bands which can be used to better interpret the structural changes occurring in DTCX upon interaction with the metal. Finally, by using the DTCX−NPs system it was possible to perform the SERS detection of PAHs directly in the Ag NPs suspension in water, which was not possible in Ag NPs functionalized with other kind of calixarenes. Thus, the combination of the good host properties of CXs and the high affinity of the DT group in the same molecule, self-assembled on

(10) Leyton, P.; Domingo, C.; Sanchez-Cortes, S.; Campos-Vallette, M.; Garcia-Ramos, J. V. *Langmuir* **2005**, *21*, 11814–11820.
(11) Leyton, P.; Sanchez-Cortes, S.; Campos-Vallette, M.; Domingo, C.; Garcia-Ramos, J. V.; Saitz, C. *Appl. Spectrosc.* **2005**, *59*, 1009–1015.
(12) Leyton, P.; Domingo, C.; Sanchez-Cortes, S.; Campos-Vallette, M.; Diaz, G. F.; Garcia-Ramos, J. V. *Vib. Spectrosc.* **2007**, *43*, 358–365.
(13) Leyton, P.; Sanchez-Cortes, S.; Garcia-Ramos, J. V.; Domingo, C.; Campos-Vallette, M.; Saitz, C.; Clavijo, R. E. *J. Phys. Chem. B* **2004**, *108*, 17484–17490.
(14) Guerrini, L.; Garcia-Ramos, J. V.; Domingo, C.; Sanchez-Cortes, S. *Langmuir* **2006**, *22*, 10924–10926.
(15) Thorn, G. D.; Ludwig, R. A. *The Dithiocarbamates and Related Compounds*; Elsevier Publishing Company: Amsterdam, The Netherlands, 1962.
(16) Sanchez-Cortes, S.; Vasina, M.; Francioso, O.; Garcia-Ramos, J. V. *Vib. Spectrosc.* **1998**, *17*, 133–144.
(17) Sanchez-Cortes, S.; Domingo, C.; Garcia-Ramos, J. V.; Aznarez, J. A. *Langmuir* **2001**, *17*, 1157–1162.
(18) Morf, P.; Raimondi, F.; Nothofer, H. G.; Schnyder, B.; Yasuda, A.; Wessels, J. M.; Jung, T. A. *Langmuir* **2006**, *22*, 658–663.

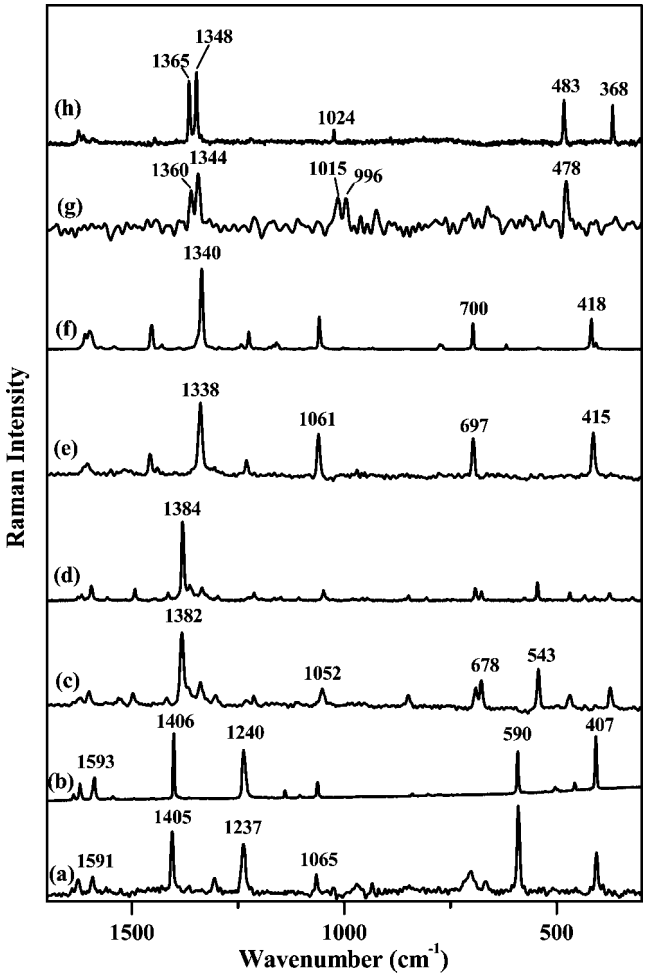

Figure 4. (b, d, f, and h) Raman spectra of PYR, BcP, TP, and COR, respectively, in the solid state. (a, c, and e) SERS difference spectra of DTCX−PAHs complexes at the concentration ratio 10^{-4} M/10^{-6} M for PYR, BcP, and TP, respectively. (g) SERS difference spectra of DTCX−COR complexes at the concentration ratio 10^{-4} M/10^{-7} M, multiplied by a factor of 5.

Table 1. Structural Marker Bands and Band Ratios Measured from the DTCX and DTCX−PAHs SERS Spectra for the Analyzed PAH Pollutants

	ν (C=N$^+$)	ν (C=S)/ν(C−S)	I_{702}/I_{665}	I_{702}/I_{571}
DTCX	1520	0.691	2.159	0.936
DTCX/PYR	1523	0.626	2.245	1.095
DTCX/BcP	1524	0.634	2.424	1.073
DTCX/TP	1523	0.649	2.639	1.250
DTCX/COR	1520	0.720	1.981	0.735

a nanostructured metal, could be a good strategy to design new sensitive and selective surfaces for the detection of PAHs. The effectiveness of such a system is evaluated in the present work.

The conformation of self-assembled calixarenes on the metal surface is a critical factor determining the host ability toward the pollutants, that is why we previously investigated the effect of the surface covering and surface properties on the geometry absorption of the DTCX molecules.[19] In the latter work, an identification of DTCX structural marker bands, related to the interaction geometry of the DT group with the metal and the conformation of the calixarene cavity, was carried out.

(19) Guerrini, L.; Garcia-Ramos, J. V.; Domingo, C.; Sanchez-Cortes, S. 2008.

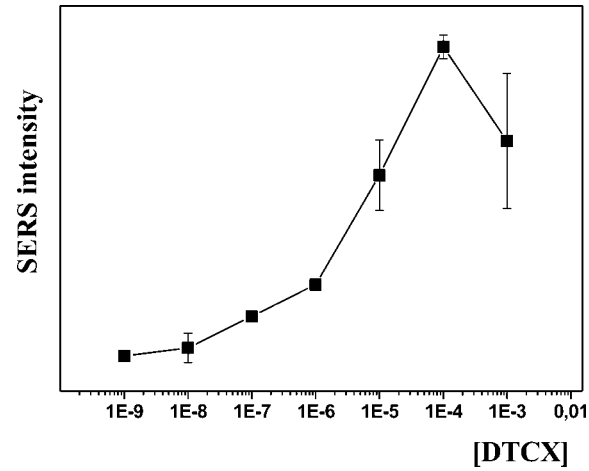

Figure 5. SERS intensity of the PYR marker band at 1405 cm^{-1} at different DTCX concentrations. In the figure, the average values as well as the quadratic standard deviation resulting from three different measurements are displayed.

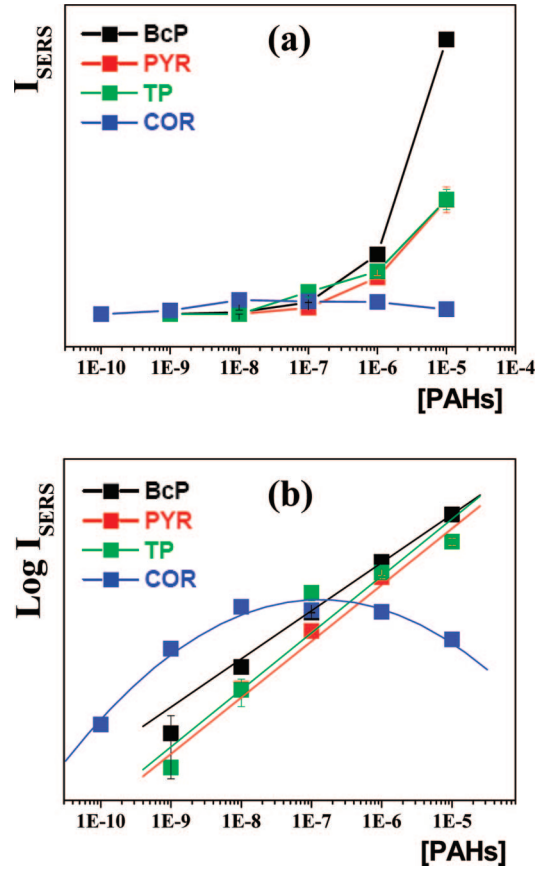

Figure 6. (a) Variation of SERS intensity of the most intense PAH bands (1405, 1382, 1338, and 1344 cm^{-1} for PYR, BcP, TP, and COR, respectively) when changing the pollutant concentration, maintaining the DTCX concentration at 10^{-4} M. (b) Logarithmic plot of I_{SERS} vs [PAHs] together with linear fitting. Average values as well as the quadratic standard deviation resulting from three different measurements are displayed.

The aim of the present paper is to systemize the application of DTCX−NPs sensing systems on the detection of PAHs in water. The sensitivity and selectivity of DTCX as the host were investigated in the detection of four different pollutants: pyrene (PYR), benzo[*c*]phenanthrene (BcP), triphenylene (TP), and coronene

Table 2. log *K*, −p*K*, *n*, and LOD Values Deduced from the Graphs in Figure 6 for the Analyzed PAHs

	log *K*″	−p*K*	*n*	LOD
BcP	8.09 ± 0.10	4.09 ± 0.10	0.71 ± 0.01	10^{-9} M (204 ppt)
PYR	7.93 ± 0.35	3.93 ± 0.35	0.72 ± 0.04	10^{-8} M (2.02 ppb)
TP	7.19 ± 0.30	3.19 ± 0.30	0.60 ± 0.12	10^{-8} M (2.04 ppb)
COR	11.13 ± 2.01	7.13 ± 2.01	0.97 ± 0.22	10^{-10} M (30 ppt)

(COR) (Figure 2). These four PAHs were selected because of their different sizes, ranging from four (PYR, BcP, TP) to seven (COR) condensed benzene-rings, and thickness. The application of SERS was aimed toward two different objectives: (a) a qualitative study of the detection of the pollutants by analyzing the structural marker bands of both the host and the ligand and (b) a quantitative analysis of the pollutants based on the SERS measurements. This could be accomplished thanks to the fact that the SERS spectra afford fingerprints of the molecular species. The quantitative application of SERS is a matter of discussion nowadays due to the relative instability of nanoparticle in suspension, affecting the intensity SERS. This is because the SERS measurements normally involve multiple phenomena: dilution, diffusion, adsorption, and partial aggregation of the metal NPs, which are difficult to control. In host functionalized NPs the further aggregation of particles is relatively avoided by large linker molecules, such as DTCX.

EXPERIMENTAL SECTION

Pyrene (PYR), benzo[*c*]phenanthrene (BcP), triphenylene (TP), and coronene (COR) (Figure 2) were purchased from Aldrich and used as received. Solutions of PYR, BcP, and TP in acetone (99%) were prepared to a final concentration of 10^{-2} M. Solution of COR in acetone (99%) was prepared to a final concentration of 10^{-4} M. The aqueous solutions were prepared by using Milli-Q water.

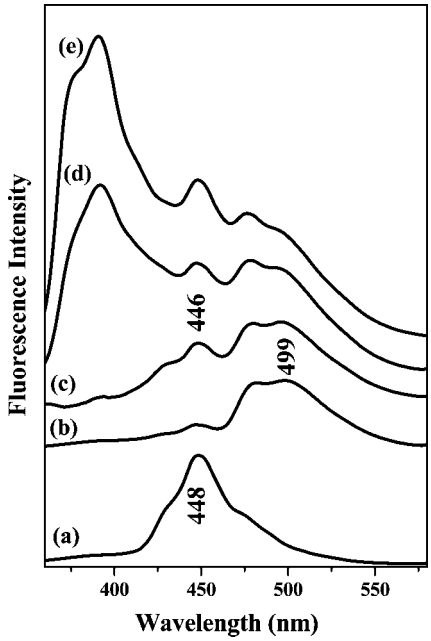

Figure 7. Fluorescence emission spectra of aqueous solutions of (a) COR 10^{-7} M, (b) COR 10^{-6} M, (c) difference spectrum (e)–(d), (d) mixture of PYR, TP, and BcP 10^{-6} M each, (e) mixture of PYR, TP, BcP, and COR, 10^{-6}M each. Excitation at 300 nm.

25,27-Diethyl-dithiocarbamic-26,28-dihidroxy-*p*-*tert*-butylcalix[4]arene (DTCX) (Figure 1a) was prepared from 25,27-diethylamino-26,28-dihidroxy-*p*-*tert*-butylcalix[4]arene (ACX) by exposing the initial amino compounds to an excess of CS_2 in methanol, following a modified method of that described by Zhao et al.[20] The exact procedure was as follows: 1 mL of a 10% solution of CS_2 in methanol was added drop by drop to 3.7 mL of a 5.0×10^{-3} M solution of ACX in methanol while stirring. The white solid obtained was washed three times with water before preparing a 5×10^{-2} M solution in acetone.

9-Methylanthracene-methyl-dithiocarbamate (MAMDT, Figure 1b) was synthesized following the same procedure as DTCX, directly from the parent amino compound. A DMSO solution of MAMDT 10^{-2} M was prepared.

Silver hydroxylamine nanoparticles (Ag NPs) were prepared by reduction of silver nitrate with hydroxylamine hydrochloride at room temperature.[21] This method leads to a more uniform distribution of size and shape together with the absence of excess citrate and its oxidation products, which could interfere with the SERS measurements.[22,23] The average size of the prepared Ag NPs was 50 nm displaying an almost spherical shape, in contrast to the particles obtained by reduction with citrate which shows a broader distribution of sizes and shapes. The Ag NPs suspension was characterized by the resonance spectra of metallic plasmons, showing a maximum at ~410 nm with an average full width at half-height (fwhh) of 80 nm. The Ag NPs were previously aggregated by adding an aliquot of potassium nitrate solution up to a final concentration of 3×10^{-2} M, and then an aliquot of DTCX in acetone (5×10^{-2} M) was added to the final desired concentration. The aggregation induced by the salt lead to a slight change of the color and a slight increase of the plasmon absorption at higher wavelengths, thus indicating that the aggregation extent is limited. The DTCX-functionalized Ag NPs were then exposed to the pollutant by adding an aliquot of the PAHs acetone solution to the desired concentration. Three spectra were measured for each sample in the quantitative treatment of both the [DTCX] and [PAH] profiles. SERS measurements of PAHs mixtures were accomplished by previously mixing the pollutants in the same acetone solutions before the addition to the DTCX functionalized NPs. Three different SERS samples were prepared to measure the SERS intensity of the PAHs shown in this work.

The normal Raman and the SERS spectra were recorded with a Renishaw Raman microscope system RM2000 equipped with a diode laser emitting at 785 nm. All Raman spectra were measured under macroconditions. Fluorescence spectra were measured with a Perkin-Elmer LS45 luminescence spectrometer.

RESULTS AND DISCUSSION

SERS of Dithiocarbamate Calix[4]arene Derivative. A detailed analysis of the adsorption and self-assembling of DTCX on Ag NPs was reported in a previous work.[19] The strong

(20) Zhao, Y.; Perez-Segarra, W.; Shi, Q. C.; Wei, A. *J. Am. Chem. Soc.* **2005**, *127*, 7328–7329.
(21) Leopold, N.; Lendl, B. *J. Phys. Chem. B* **2003**, *107*, 5723–5727.
(22) Sanchez-Cortes, S.; Garcia-Ramos, J. V. *J. Raman Spectrosc.* **1998**, *29*, 365–371.
(23) Canamares, M. V.; Garcia-Ramos, J. V.; Gomez-Varga, J. D.; Domingo, C.; Sanchez-Cortes, S. *Langmuir* **2005**, *21*, 8546–8553.

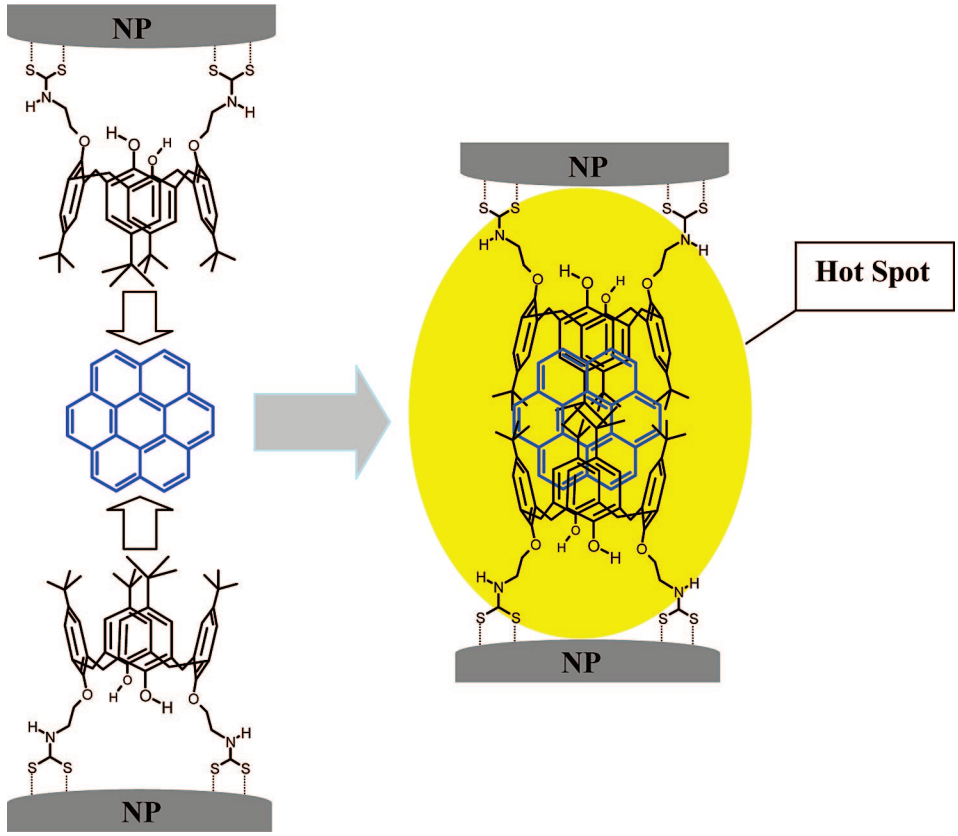

Figure 8. Scheme showing the COR−DTCX complexation mechanism with formation of the highly sensitive interparticle junction.

adsorption of the DTCX on the NP surface takes place through the S atoms inducing a transformation of the DT group into the corresponding thioureide form[15−17,19] revealed by the new band around 1520 cm^{-1} attributed to stretching of the partial C=N^+ double bond (Figure 1c). The SERS spectrum of DTCX is dominated by the DT bands seen at 1022 and 966 cm^{-1} that have been ascribed to the υ(C=S) and to υ(C−S) motions, respectively (Figure 3a). The analysis of the above bands allows one to distinguish between a monodentate or a bidentate interaction with the metal.[19] The larger the intensity ratio $I_{\upsilon(C=S)}/I_{\upsilon(C-S)}$ and the lower the wavenumber peak position of the thioureide band, the more abundant the monodentate form will be.

On the other hand, other bands related to the benzene rings afford information about the host cavity, the conformation of these rings, and the orientation relative to the metal surface. For instance, the intensity of the 702/665 cm^{-1} doublet is related to changes in the cavity conformation, as the intensity ratio of these two bands is sensitive to the surface coverage of DTCX[15−17,19] and the interaction of DTCX with pyrene.[14] This is supported by the fact that these bands are assigned to in-plane structural motions of the aromatic moieties,[24] probably coupled to ring substituents, and also by the fact that they were not seen in the SERS of DT.[16] In fact, the 702 cm^{-1} band has been ascribed to the ring breathing band.[25] Thus, the I_{702}/I_{665} ratio can be considered as a marker parameter of the cavity conformation.

The band at 571 cm^{-1}, attributed to skeletal in-plane band coupled to ring−CO deformations,[24,26−29] undergoes a marked decrease in relation to that at 702 cm^{-1}, upon adsorption of DTCX and other calix[4]arenes.[13] This weakening is further intensified by increasing the surface covering on the Ag NPs and when pollutants interact with the calixarene. These changes can be attributed to a reorientation of the benzene rings on the surface, in such a way that the increase of the I_{702}/I_{571} ratio is related to a more perpendicular orientation of the benzene rings. In summary, the conformational state of the aromatic intramolecular cavity can be monitored by measuring the I_{702}/I_{665} ratio, and the orientation of aromatic benzene rings with respect to the surface can be followed by analyzing the I_{702}/I_{571} ratio. The smaller the I_{702}/I_{665} ratio, the closer the calixarene cavity, and the larger the I_{702}/I_{571} ratio, the more perpendicular the orientation of the benzene rings on the metal surface. Indeed, these two parameters are related, as the closer is the interaction cavity, the higher is the perpendicular orientation of the benzene rings delimiting this cavity.

SERS Analysis of DTCX−PAHs Complexes. Featureless spectra are obtained when acetone solutions of all the PAHs assayed in this work were added to the colloidal suspension in the absence of DTCX functionalization. Our experience indicates

(24) Katsyuba, S.; Chernova, A.; Schmutzler, R. *Org. Biomol. Chem.* **2003**, *1*, 714–719.
(25) Moreira, W. C.; Dutton, P. J.; Aroca, R. *Langmuir* **1995**, *11*, 3137–3144.
(26) Kondyurin, A.; Rautenberg, C.; Steiner, G.; Habicher, W. D.; Salzer, R. *J. Mol. Struct.* **2001**, *563*, 503–511.
(27) Katsyuba, S.; Chernova, A.; Schmutzler, R.; Grunenberg, J. *J. Chem. Soc., Perkin Trans. 2* **2002**, 67–71.
(28) Katsyuba, S. A.; Grunenberg, J.; Schmutzler, R. *J. Mol. Struct.* **2001**, *559*, 315–320.
(29) Katsyuba, S. A.; Schmutzler, R.; Hohm, U.; Kunze, C. *J. Mol. Struct.* **2002**, *610*, 113–125.

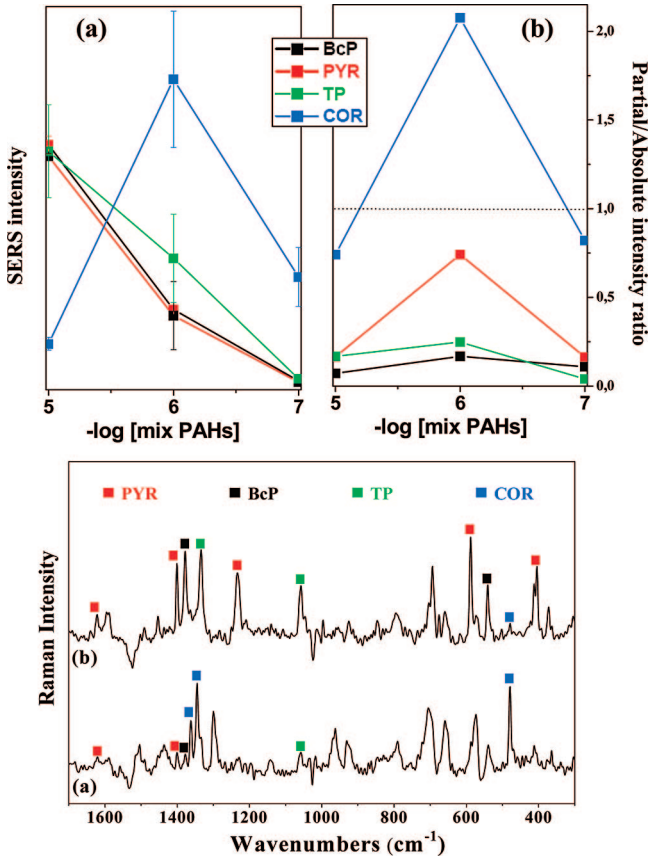

Figure 9. Top panel: (a) Partial SERS intensity of the 1405 cm^{-1} PYR band, 1382 cm^{-1} BcP band, 1338 cm^{-1} TP band, and 1344 cm^{-1} COR band at different PAHs concentration. (b) Partial/absolute SERS intensity ratio: the average values as well as the quadratic standard deviation corresponding to three measurements are displayed. Bottom panel: SERS difference spectra DTCX/totalPAHs − DTCX measured at the following concentration ratios (a) 10^{-4} M/10^{-6} M and (b) 10^{-4} M/10^{-5} M, displaying Raman features corresponding to all the PAHs contained in the mixture.

that even when depositing an aliquot of a PAH solution on metal-island films, the molecule is not actually adsorbed once the solvent is evaporated because the PAH molecules remain as microcrystals. The high polar nature of the Ag NPs in suspension makes the adsorption of highly apolar PAHs molecules difficult.

On the contrary, when PAH solutions were added to the DTCX functionalized Ag NPs, intense Raman bands of PAHs appear, as illustrated in Figure 3 for the case of BcP. As can be seen in Figure 3b, the SERS spectrum of the DTCX−BcP complex is integrated by a mixture of both DTCX and the pollutant bands, revealing strong spectral changes in both species. The observation of BcP features is indeed attributed to the formation of a host−guest complex with DTCX (Figure 3, top scheme).

A control experiment was accomplished by using MAMDT-functionalized AgNPs. The SERS spectrum of MAMDT (Figure S1, see the Supporting Information) also reveals an intensification of DT bands, with a predominance of bidentate molecules adsorbed onto the surface. In contrast to what happens in DTCX, whose aromatic groups are placed much further to the surface, the still intense anthracene bands indicate a perpendicular orientation with respect to the surface and a relative proximity of this moiety to the metal. However, no SERS bands of the pollutant can be detected in this case likely due to the absence of cavities in this system. One of the main advantages of the analysis of PAHs by SERS is the possibility of investigating the structural changes occurring in both the host and guest molecules as a consequence of the interaction verified on the metal surface.

For a better study of the influence of DTCX on the pollutant structure, difference spectra (DTCX/PAH−DTCX) were obtained for all the analyzed PAHs (Figure 4). The comparison with the corresponding Raman of solids revealed significant differences due to the interaction with the host. In general terms, an intensification is observed for certain bands corresponding to symmetric a_g modes[30−32] (e.g., bands at 590 cm^{-1} in PYR, 678 and 543 cm^{-1} in BcP, 697 cm^{-1} in TP, and at 478 cm^{-1} in COR). This effect is associated with an enhancement through a Franck−Condon resonance mechanism.[33] On the basis of the above results, we have deduced a host−guest interaction mechanism through $\pi-\pi$ stacking between the aromatic systems of DTCX and PAHs leading to the formation of a charge-transfer complex.[13] It should be noted that for the case of COR, the largest spectral changes were observed. This pollutant undergoes a general shift downward of the majority of bands, and there is a disappearance of the bands at ∼1600 cm^{-1} and 368 cm^{-1} and the appearance of a new feature at 996 cm^{-1}.

A structural analysis of DTCX was also made on the basis of the SERS spectra. This was accomplished by following the structural marker bands and band ratios deduced from the SERS of DTCX shown in the last section, which are related to the DTCX−metal interaction geometry and the internal cavity conformation of the host. These structural parameters are influenced by the interaction with PAH molecules and their values are listed in Table 1 in comparison to free DTCX.

As can be seen, the structural markers associated with the DTCX binding to the metal ($\upsilon C{=}N^+$ and $I_{\upsilon(C=S)}/I_{\upsilon(C-S)}$ ratio) indicate an increase of the bidentate interaction of the calixarene with the surface when the DTCX−PAH complex is formed. This is probably related to a strengthening of the interaction of the host with the metal, as a consequence of the PAH to DTCX charge-transfer. COR is an exception to this behavior. However, the structural changes induced by the union to PAHs are much lower that those observed upon modification of the calixarene surface coverage or by changing the metal NPs preparation protocol.[19]

Concerning the I_{702}/I_{665} and I_{702}/I_{571} ratios, slight changes can also be detected in such a way that an increase of these two parameters is observed in the direction PYR → BcP → TP. This result suggests a change in the intramolecular cavity which seems to adopt a closer conformation in the presence of the guest, resulting in a more perpendicular orientation of the benzene rings with respect to the surface as illustrated in Figure 3, top scheme. COR is again an exception to this rule, as a relative decrease of these ratios is seen in relation to the free DTCX. This effect is likely due to the bigger size of COR, which may induce an opening of the DTCX cavity.

(30) Hudgins, D. M.; Sandford, S. A. *J. Phys. Chem. A* **1998**, *102*, 329–343.
(31) Shinohara, H.; Yamakita, Y.; Ohno, K. *J. Mol. Struct.* **1998**, *442*, 221–234.
(32) Carrasco-Flores, E. A.; Clavijo, R. E.; Campos-Vallette, M. M.; Aroca, R. F. *Appl. Spectrosc.* **2004**, *58*, 555–561.
(33) Creighton, J. A. The Selection Rules for Surface-Enhanced Raman Spectroscopy. In *Spectroscopy of Surfaces*; John Wiley & Sons: New York, 1988.

Quantitative Analysis of DTCX−PAHs Complexes. In order to identify the optimum DTCX surface coverage for the detection of PAHs, SERS spectra of the DTCX−PYR complex were collected by varying the concentration of the host, ranging from 10^{-3} to 10^{-9} M, while the PYR concentration was kept constant at 10^{-6} M. In Figure 5, the intensity of PYR marker SERS band at 1405 cm^{-1} at different DTCX concentrations is plotted.

When increasing the DTCX surface coverage the number of host cavities available for the PYR complexation grows, but the cavities simultaneously adopt a closer configuration at higher concentration,[19] which in turn reduces the efficiency of the host−guest interaction. Furthermore, a very high concentration of DTCX may provoke other undesired phenomena as multilayer deposition and massive aggregation of the colloidal NPs. The maximum of PYR signal appearing at 10^{-4} M of DTCX in the colloidal suspension likely corresponds to the best compromise between these two opposite effects, i.e., maximum coverage with the lower effect of multilayer DTCX adsorption.

Figure 6a illustrates the SERS intensity of the most intense PAH bands (1405, 1382, 1338, and 1344 cm^{-1} for PYR, BcP, TP, and COR, respectively) when changing the pollutant concentration, while the DTCX concentration was kept constant at 10^{-4} M for all measurements. Figure 6b display the corresponding plots of log I_{SERS} vs log[PAH], where I_{SERS} is the SERS intensity registered for the PAH bands above. As can be seen, all the plots can be fitted to a linear graph except for COR, for which a curve is obtained. Assuming an interaction between DTCX and n molecules of PAH, the following equilibrium can be considered:

$$K' = \frac{[\mathrm{DTCX/PAH}_n]}{[\mathrm{DTCX}][\mathrm{PAH}]^n} \quad (1)$$

and then

$$\log[\mathrm{DTCX/PAH}_n] = \log K'[\mathrm{DTCX}] + n \log[\mathrm{PAH}] \quad (2)$$

Now we can assume that the only contribution to I_{SERS} of PAHs is provided by those PAH molecules interacting with the host. Thus, $I_{SERS} = C[\mathrm{DTCX/PAH}]$, where the constant C includes all the physical constant and parameters related to the Raman emission and SERS enhancement which are not related to the emitting molecule concentration. Since [DTCX] was maintained constant (10^{-4} M), eq 2 can be rewritten as

$$\log I_{SERS} = \log K'' + n \log[\mathrm{PAH}]$$

with

$$K = K' C[\mathrm{DTCX}] \quad (3)$$

Thus a binding constant between DTCX and PAH, K, can be defined as $K = K'C = K''[\mathrm{DTCX}]$. This constant and n (number of PAH molecules bounded to a DTCX) can be deduced from the linear graphs plotted in Figure 6b. In Table 2, the values calculated for log K ($-$pK), and n as well as the measured limit of detections (LODs) are shown for all the analyzed PAH. From these values we can deduce that the number of PAH bounded to each DTCX host can be approximated to 1, while the affinity of the binding to DTCX increases in the following order: TP < PYR < BcP < COR. The LOD was also measured for all the pollutants (Table 2). As can be seen, the PAHs marker bands are observed for concentrations as low as 10^{-8} M in the case of PYR and TP, 10^{-9} M in the case of BcP, and 10^{-10} M in the case of COR. These LODs are similar to those reported elsewhere in the analysis of PAHs by chromatographic and fluorimetric methods.[34−37]

For the PAHs bearing four benzene rings, one can see that the affinity is higher in the case of BcP, whereas the TP guest seems to induce the larger modification of the calixarene cavity. Thus, the accommodation of each adsorbed analyte on the host molecule is not equivalent. Most probably, the high affinity of BcP to bind DTCX regarding the other four-ring PAHs is associated with the existence of a "fiord" moiety in this molecule (Figure 2) which makes the BcP structure twisted from planarity[9] and, thus, more suitable for the positioning inside the calixarene cavity. Besides, the planar structure of TP, together with the existence of more free external benzene rings, may be the reason why the calixarene cavity adopts a closer and tighter structure in DTCX−TP complex. Finally, the larger size of COR leads to a further opening of the DTCX cavity as revealed by structural parameters in Table 1.

COR also represents an exception regarding the other investigated PAHs when analyzing the I_{SERS} vs [COR] plot (Figure 6b). In fact, I_{SERS} increases for low COR concentrations and, then, decreases at pollutant concentrations above $10^{-7}/10^{-8}$ M. The binding affinity of COR was deduced for the data measured at low concentrations and results were much higher than the other PAHs. This striking behavior correlates well with the opposite effect induced by COR on the DTCX structure, as compared to the other PAHs (see structural parameters deduced from SERS spectra in Table 1). The intensity decrease seen for COR at high concentration can be associated to its extremely low solubility in water (5×10^{-9} M), more than 2 orders of magnitude smaller than the solubilities of PYR, BcP, and TP.[38] Thus, above a concentration of 10^{-8} M, COR undergoes a self-aggregation which seriously limits its binding to DTCX. This self-aggregation can be demonstrated by fluorescence spectroscopy (Figure 7). The fluorescence emission spectra of COR aqueous solutions reveal that upon increasing of the COR concentration from 10^{-7} to 10^{-6} M (Figure 7a and b, respectively), the dominating monomer emission band at 448 nm becomes much weaker, while a new band appears at 499 nm assigned to the excimer band resulting from the aggregation of COR.[39]

The accommodation of each adsorbed analyte into the host molecule is not equivalent and is largely determined by the host

(34) Bourdat-Deschamps, M.; Daudin, J. J.; Barriuso, E. *J. Chromatogr., A* **2007**, *1167*, 143–153.
(35) Zuazagoitia, D.; Millan, E.; Garcia, R. *Chromatographia* **2007**, *66*, 773–777.
(36) Cai, Z. Q.; Zhu, Y. X.; Zhang, Y. *Spectrochim. Acta, Part A* **2008**, *69*, 130–133.
(37) Lopes, W. A.; da Rocha, G. O.; Pereira, P. A. D.; Oliveira, F. S.; Carvalho, L. S.; Bahia, N. D. C.; Conceicao, L. D.; de Andrade, J. B. *J. Sep. Sci.* **2008**, *31*, 1787–1796.
(38) NIST Scientific and Technical Database.
(39) Seko, T.; Ogura, K.; Kawakami, Y.; Sugino, H.; Toyotama, H.; Tanaka, J. *Chem. Phys. Lett.* **1998**, *291*, 438–444.

and the guest volumes.[40] Therefore, we may suppose that COR molecules, because of their larger size compared to the other PAHs under investigation, can induce the formation of host−guest complexes where the pollutant acts as a bridge between two DTCX molecules. The resulting capsule-like inclusion would locate the COR right at the gap between the two NPs, as illustrated in Figure 8. This supramolecular assembly brings about interparticle junctions or gaps, where the electromagnetic field is significantly enhanced (it is estimated to be $\sim 10^3$ times greater than the rest of the surface in the case of interparticle distances of 2−3 nm[41,42]). These gaps were also called hot spots. The organization of the DTCX−COR−DTCX complex accounts both for the extremely low LOD value deduced for COR and the strong effect of complexation on the COR structure, as deduced from the SERS spectra.

Finally, DTCX-functionalized Ag NPs were also applied in the detection of PAH mixtures at different partial concentrations (10^{-5}, 10^{-6}, and 10^{-7} M) of each pollutant. Strong SERS features of all analyzed PAHs were also measured in this case (Figure 9, bottom panel). The intensities corresponding to each PAH molecule (named as partial intensities to distinguish them from the absolute ones reported in Figure 6a) are plotted in Figure 9a. Moreover, Figure 9b shows the ratio between the partial and the absolute SERS intensity of each pollutant. It is worth noting that while COR underwent a marked SERS intensity increase in the presence of the other PAHs (approximately its SERS intensity is 2-fold that observed in the absence of other PAHs at a partial concentration of 10^{-6} M), marked SERS intensity decreases were observed in the case of PYR, BcP, and TP.

The SERS intensity weakening detected for BcP, PYR, and TP in the presence of COR was attributed to the higher affinity of COR to interact with DTCX. This effect is reinforced by the fact that each DTCX−COR−DTCX complex lead to the formation of interparticle hot spots, where the SERS intensity is expected to be higher. The lower effect on PYR, especially at an overall concentration of 10^{-6} M, suggests that DTCX−PYR−DTCX could also occur although at a lower extent in relation to COR. For higher concentrations of the total PAHs (mixture of 10^{-5} M each pollutant), a general decrease of the SERS intensity is seen (Figure 9b) because other phenomena such as PAHs aggregate formation or a multilayer effect may occur to a larger extent, resulting in the reduction of the corresponding SERS signals. Therefore, the multicomponent analysis of PAHs by SERS depends on different factors which should be better studied in future works.

On the other hand, the great intensification of COR SERS signal in the mixture could be again associated to the solubility of COR. Figure 7 displays the fluorescence spectra of the PAHs mixture (10^{-6} M for each PAH) in water in the absence (Figure 7d) or presence (Figure 7e) of COR. The difference spectrum (Figure 7c) reveals a monomer band at 446 nm which is approximately 6 times stronger than the corresponding monomer band appearing in the emission spectrum of 10^{-6} M COR in water solution (Figure 7b). In contrast, the excimer emission band (at 499 nm) undergoes a significant intensity decrease. Therefore, the presence of the other PAHs increases the actual concentration of the COR by increasing the number of monomers, thus accounting for the SERS intensity increase observed in the mixture. This result is of great importance as COR is usually accompanied by other pollutants in the environment.

CONCLUSIONS

The functionalization of Ag nanoparticles with a dithiocarbamate calix[4]arene host (DTCX) rendered a sensitive and selective system in the detection of PAHs. The SERS spectra not only afforded information about the existence of the pollutant but also revealed important structural information from both the host and the analyte which was crucial to understand and deduce the different interaction occurring in the two molecular systems once the complex was formed. From this analysis, a host−guest interaction mechanism through $\pi-\pi$ stacking between the aromatic systems of DTCX and PAHs leading to the formation of a charge-transfer complex can be deduced. The analysis of the SERS spectrum of DTCX revealed marker bands associated with the DTCX binding to the metal ($\upsilon C{=}N^+$ and $I_{\upsilon(C=S)}/I_{\upsilon(C-S)}$ ratio), which indicate an increase of the bidentate interaction of the calixarene adsorbed on the surface when the DTCX−PAH complex is formed. The I_{702}/I_{665} and I_{702}/I_{571} ratios are structural marker parameters related to the intramolecular cavity, which seems to adopt a closer configuration in the presence of the guest, thus adopting a more perpendicular orientation of the benzene rings with respect to the metal surface.

The affinity constants and the limits of detection of PAHs containing four benzene rings (BcP, PYR, and TP) indicate that these molecules have a similar behavior regarding the interaction with the calixarene (marked structural change on the calixarene host, similar affinity constant and limit of detection ranging in the $10^{-7}-10^{-8}$ interval). COR represents a special case. The higher affinity of this analyte in relation to DTCX and the lower influence on the calixarene structure lead us to suggest an interaction mechanism with the host involving two calixarene molecules and the formation of interparticle hot spots, where the sensitivity is highly enhanced.

Finally, the multicomponent analysis of PAH mixtures by SERS implies a deep study of the affinity constant modification in the presence of other species. However, this work represented a first step in the analysis of PAHs by DTCX−Ag systems and a first approach to apply these systems for the multicomponent analysis of PAHs mixtures without a previous separation of pollutants.

ACKNOWLEDGMENT

The authors acknowledge Dirección General de Investigación (Ministerio de Educación y Ciencia) Project Number FIS2007-63065 and Comunidad Autónoma de Madrid Project Number S-0505/TIC/0191 MICROSERES for financial support. L.G. acknowledges CSIC for an I3P fellowship.

SUPPORTING INFORMATION AVAILABLE

Additional information as noted in text. This material is available free of charge via the Internet at http://pubs.acs.org.

(40) Rudkevich, D. M. *Calixarenes 2001*; Kluwer Academic: Dordercht, The Netherlands, 2001.
(41) Moskovits, M. *Rev. Mod. Phys.* **1985**, *57*, 783–826.
(42) Le Ru, E. C.; Etchegoin, P. G.; Meyer, M. *J. Chem. Phys.* **2006**, 125.

Received for review August 14, 2008. Accepted December 6, 2008.

AC801709E